Engineering and Technology Journal e-ISSN: 2456-3358

Volume 09 Issue 05 May-2024, Page No.- 3988-3999

DOI: 10.47191/etj/v9i05.16, I.F. – 8.227

Utilization of Geothermal Fluid as a Heat Source for Absorption Refrigeration System for Food Preservation – A Case of Bwanda and Gwisho Hotsprings

Kabalu Wamunyima[1], Edwin Luwaya[2]

[1,2] School of engineering, University of Zambia

ABSTRACT: Zambia has significant geothermal resources with over 86 hotsprings identified. Installation of a 250kW off-grid pilot binary-cycle power plant is currently underway at the Bwanda and Gwisho goethermal site. It is estimated that there is 90,000 herd of cattle in the villages around the pilot power plant. Little milk from these herds of cattle reaches the market due to scarce collection points with cooling facilities. This study assesses the applicability of utilizing exhaust geothermal fluid from a binary-cycle geothermal power plant for powering an absorption refrigeration system (ARS) for storing food, specifically milk. Two absorption systems; Lithium Bromide-water and the ammonia-water ARS are compared. The COPs, energy input and mass flowrates required to produce various cooling loads (40kW – 160kW) are compared. The results show that the exhaust geothermal fluid energy (504kW) is sufficient for powering both ARSs for storing milk to its suitable storage temperature of 4^{o}C. The results also show that the Lithium Bromide-water system is more suitable for this application, because it produces a higher maximum COP (0.76) compared to the ammonia-water system's maximum COP (0.64), it produces a higher maximum cooling capacity (380kW) compared to the ammonia-water systems maximum capacity (216kW). It requires lower input mass flowrate and pump work at all cooling capacities (40kW – 160kW). Therefore, a Lithium Bromide-water absorption chiller for storing the amounts of milk currently collected in the study area is designed. Optimized design specifications are provided.

KEYWORDS: Absorption refrigeration, binary cycle plant, cooling capacity, geothermal energy and exhaust geothermal fluid.

1. INTRODUCTION

Recently the utilization of all available renewable energy resources in a smart way have been given great attention. This has been mainly due to their contribution towards reducing the reliance on fossil fuels which contribute massively to global warming. Electricity generation through renewable sources of energy is expected to continue growing, as nations increase efforts towards achieving net zero emissions by 2050. One such renewable energy source which shows great promise is geothermal energy. Many studies have been done on how geothermal energy can be utilized directly and indirectly. Other efforts have also been made to advantageously utilize waste and un-utilized geothermal energy.

Geothermal energy is renewable and sustainable energy that can be utilized directly or indirectly. Electricity generation is one common way of indirectly utilising geothermal energy. For the recorded geothermal resources in Zambia, the binary cycle power system is the most applicable for electricity generation. Binary cycle geothermal power plants produce low grade thermal energy which is considered as wasted energy, awaiting further utilization or reinjection back into the reservoir. Depending on its energy content, this lower grade thermal energy can be used to power heat driven processes such as district heating, hot baths and drying and cooling processes. Absorption refrigeration systems are cooling processes which need thermal energy as a necessary condition for producing a refrigeration effect.

There are significant but under-explored and under-exploited geothermal resources in Zambia. The geological survey's 1974 reconnaissance of Hot and mineralised springs identified 86 hot springs, all of which are hosted in fault systems within Proterozoic basement rocks and associated mainly with the Karoo (Permian) era basin [1]. The capacity of known geothermal systems in Zambia's Karoo Basins is estimated to be greater than 1000 MW [1]. Despite all the geothermal resources, there is currently no geothermal power plant operating in Zambia. Recently, Kalahari GeoEnergy Ltd conducted systematic explorations of the Bweengwa geothermal system which houses the Bwanda and Gwisho hotsrprings within the Kafue Rift in the Southern Province. This involved extensive geophysics, engineering and drilling of 21 wells. The explorations found that the average temperature of production wells are conducive for developing low to medium enthalpy geothermal resources. Kalahari geoenergy Ltd are currently installing a 250kW off-grid binary-cycle pilot power plant. The design specifications of the power plant are such that; input geothermal fluid

temperature and mass flowrate are 108ºC and 6.2kg/s respectively. The outlet geothermal fluid temperature and mass flowrate are 80.5ºC and 6.2kg/s respectively. This source of in-expensive heat energy make absorption refrigeration systems (ARSs) economically attractive [2]. It is estimated that there is 90,000 herd of cattle in the villages around the pilot power plant. Little milk from these herds of cattle reaches the market due to scarce collection points with cooling facilities. Milk produced on-farm with minimal bacterial contamination can be successfully stored at 2°C and 4°C for up to 96 h with little effect on its microbial quality [3]. A geothermal absorption refrigeration system using geothermal fluid waste energy as the heat source could provide an option for low cost cooling systems for preserving milk in remote areas. This study aims to assess the applicability and performance of absorption refrigeration systems which use exhaust geothermal fluid as a heat source for preserving food, specifically milk. It assesses and compares the performance two absorption refrigeration systems; Lithium Bromide-water (LiBr-H_2O) and Ammonia-water (NH_3-H_2O) refrigeration systems. A suitable ARS system is selected and designed to store the amounts of milk currently collected in the study area. Simulations are run in a software called Engineering Equation Solver (ESS) in order obtain optimized design features.

2. Methodology and ARS modelling

The research design that was adopted in this study was the cross sectional study design as it involved only one contact with the study population. This design is useful in obtaining an overall 'picture' as it stands at the time of the study [4]. The study employed quantitative data collection methods through the use of direct observation. After the data was collected, thermodynamic analysis of each component of both a LiBr-water ARS and NH3-water ARS with the help of Engineering Equation Solver (EES) software was done. The heat exchanger analysis was done using the Log mean temperature difference (LMTD). The same software was used to run simulations in order to obtain optimum design features for the favourable ARS.

The following main components of the research design were identified conducted.

2.1 Determination of the maximum amount of milk collected in the study area daily.

This was done by collecting data from milk collectors in the study area.

2.2 Determination of the maximum energy contained in exhaust geothermal fluid from a binary cycle power plant.

This was done using the equations below;

$\dot{Q} = \dot{m}c(T_{in} - T_{out})$

$\dot{Q} = \dot{m}h_{in} - \dot{m}h_{out}$

2.3 Assessment of the practicability of using the energy contained in exhaust geothermal fluid to power a LiBr-water ARS and a NH_3-water ARS for cooling the amounts of milk collected in the study area daily.

To assess the practicability of using the exhaust geothermal fluid energy to power both absorption systems for cooling the amounts of milk collected in the study area. Two ARS internal models were calculated and analysed in EES. EES provides built-in thermodynamic and transport property functions for hundreds of fluids, including water, dry and moist air, most refrigerants, cryogens, and others. Included in the property database are thermodynamic properties for lithium-bromide/water and ammonia/water mixtures.

The models are calculated and analysed with the following assumptions:

1. Steady-state operating conditions.
2. No pressure drop in the pipes.
3. Heat exchangers are adiabatic.
4. No LiBr crystallization in the LiBr-H_2O system.

2.3.1 Single effect Lithium bromide/water absorption system

A systematic procedure which breaks down the larger task into a series of steps which can be checked individually, recommended by K. E Herold et al is used to model this system. The formulation of the model is based on Figure 2.1.

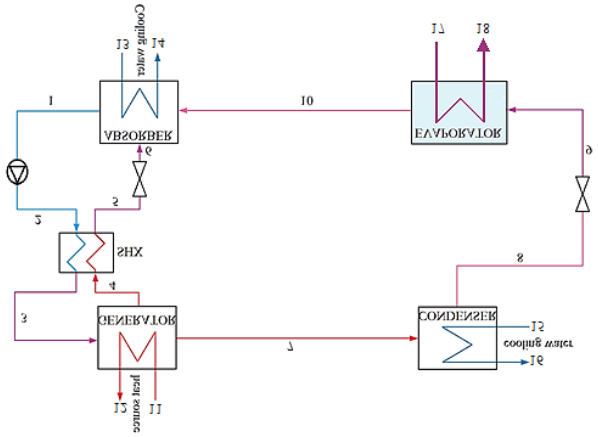

Figure 2.1

Mass balance

The mass balance formulation is summarized below.

Specified mass fraction	**Specified mass flowrate**
$x_1 = 0.55$	$\dot{m}_1 = 0.5 kg/s$
$x_2 = 0.60$	

Component	**Overall mass**	**LiBr mass**
Absorber	$\dot{m}_1 = \dot{m}_{10} + \dot{m}_6$	$\dot{m}_1 x_1 = \dot{m}_6 x_6$
Generator	$\dot{m}_4 + \dot{m}_7 = \dot{m}_3$	$\dot{m}_4 x_4 = \dot{m}_3 x_3$
Condenser	$\dot{m}_8 = \dot{m}_7$	$x_8 = x_7$
Refrig. Valve	$\dot{m}_9 = \dot{m}_8$	$x_9 = x_8$
Evaporator	$\dot{m}_{10} = \dot{m}_9$	$\dot{m}_{10} = \dot{m}_9$
Pump	$\dot{m}_2 = \dot{m}_1$	$\dot{m}_2 = \dot{m}_1$
Solution valve	$\dot{m}_6 = \dot{m}_5$	$\dot{m}_6 = \dot{m}_5$
SHX cold side	$\dot{m}_3 = \dot{m}_2$	$x_3 = x_2$
SHX hot side	$\dot{m}_5 = \dot{m}_4$	$x_5 = x_4$

Temperature inputs

The temperature inputs are used in each of the corner components. These inputs are summarized below along with how they are used in the model.

Temperature Inputs	**Saturation relation**	**Effects on model**
Aqueous LiBr states		
Absorber outlet temperature ($T_1 = 30^oC$)	$T_1 = T_{sat}(P_L, x_1)$	Sets x_1
Generator outlet temperature ($T_4 = 65^oC$)	$T_4 = T_{sat}(P_H, x_4)$	Sets x_4
Pure water states		
Condenser outlet temperature ($T_8 = 30^oC$)	$T_8 = T_{sat,\ liquid}(P_H)$	Sets P_H
Evaporator outlet temperature ($T_{10} = 2^oC$)	$T_{10} = T_{sat,\ vapor}(P_L)$	Sets P_L

Energy balances

The approach is to build on the previous computer program as a starting point for the next step. Therefore, the results from the previous solution are needed for the energy balances. The energy balance formulation for all of the main components are summarized below.

Component	**Energy balance**
Absorber	$\dot{Q}_a = \dot{m}_1 h_1 + \dot{m}_{10} h_{10} + \dot{m}_6 h_6$
Generator	$\dot{Q}_g = \dot{m}_4 h_4 + \dot{m}_7 h_7 + \dot{m}_3 h_3$
Condenser	$\dot{Q}_c = -\dot{m}_8 h_8 + \dot{m}_7 h_7$
Refrig. Valve	$h_9 = h_8$
Evaporator	$\dot{Q}_e = \dot{m}_{10} h_{10} - \dot{m}_9 h_9$
Pump	$\dot{W} = \dot{m}_2 h_2 - \dot{m}_1 h_1$
Solution valve	$h_6 = h_5$
SHX cold side	$\dot{Q}_{shx} = \dot{m}_3 h_3 - \dot{m}_2 h_2$
SHX hot side	$\dot{Q}_{shx} = -\dot{m}_5 h_5 + \dot{m}_4 h_4$

Some enthalpy terms are included and the specific enthalpy values need to be related to the other state-point variables, as indicated below.

State point	**Enthalpy relation**
Aqueous LiBr solution states	
1	$h_1 = h(T_1, x_6)$
2	$h_2 = h(T_2, x_2)$
3	$h_3 = h(T_3, x_3)$

4 $h_4 = h(T_4,x_4)$
5 $h_5 = h(T_5,x_5)$
6 $h_6 = h(T_6,x_6)$

Pure water states

7 $h_7 = h(T_7,P_6)$ Superheated water vapor
8 $h_8 = h_{sat,v}$ (T_8) Assumed to be saturated liquid
9 $h_9 = h(P_L,Q_9)$ Vapor/liquid two-phase state
10 $h_{10} = h_{sat,v}(T_{10})$ Assumed to be saturated vapor

The Models for solution heat exchanger heat transfer, temperature of vapor at outlet of desorber, and a pump model are summarized below. When these equations are added to the model, the software (EES) converges and gives the solution. Variable limits on the vapor quality Q_9 were set to restrict it to be between 0 and 1 to get it to converge.

Model	**Comments**
Solution heat exchanger, $\varepsilon = \frac{T_4 - T_5}{T_4 - T_2}$	1. Need to specify value for ε. 2. Temperature formulation works because generator outlet always has the minimum capacitance in such a cycle.
Generator outlet temperature, $T_7 = T_{sat}(x_3,P_H)$	Vapor leaving generator is assumed in equilibrium with incoming solution stream concentration (state 3). This is a standard assumption that represents the best possible case.
Pump model, $h_2 = h_1 + v_1\Delta P$	Isentropic pressure change on an incompressible fluid. Standard pump model for a liquid.

2.3.2 Single effect Ammonia/water absorption

Another step-by-step procedure recommended by K. E Herold et al is used to model a single effect Ammonia/water absorption refrigeration system, in the same computer software; Engineering Equation Solver (EES).

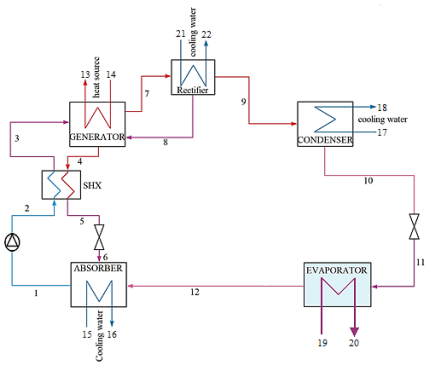

Figure 2.2

The formulation is based on Figure 2.2. In this formulation, it is assumed that the pump efficiency is 100% and that the effectiveness of the solution heat exchanger is 80%. This modelling process begun by specifically entering the unit system to be used. This is done with the $UnitSystem directive. Referring to Figure 2.2 for the locations of states, the temperatures at state 11 is –10°C, and the temperature at both states 1 and 10 is 30°C. The ammonia mass fraction at state 9 is 0.9996. The quality of the state 11 is 0.975. The quality at states 1, 8, and 10 is 0 (liquid), and it is 1 (vapor) at states 7 and 9. The solution mass flow rate driven by the pump was varied, and the effectiveness of the solution heat exchanger is 0.8. The pump is assumed to be isentropic. We know the difference between the ammonia mass fractions at states 1 and 4 is 0.1.

The pressure losses in the cycle are neglected, therefore, there are only two pressure levels in this cycle, and pressure drops occur only across the valves. The low pressure is fixed by the saturation conditions at the evaporator exit (state 11), which is known through property relations since the temperature, overall mass fraction, and quality at state 11 are specified.

$P_1 = P_6 = P_{12} = P_{13} = P_{sat}(T_{12}, x_{12}, Q_{12})$

The high pressure is fixed by the saturation conditions at the condenser exit (state 10).

$P_2 = P_3 = P_4 = P_5 = P_7 = P_8 = P_9 = P_{10} = P_{sat}(T_{10}, x_{10}, liq)$

The ammonia mass fractions throughout the absorption cycle are determined by the operating conditions, and they fluctuate to match the conditions. The mass fractions of the ammonia-poor stream (states 1, 2, and 3) depend on the given absorber temperature and the evaporator pressure. The mass fractions of the ammonia-rich stream (states 4, 5, and 6) depend on the specified difference between the rich and poor streams. The governing equations consisting of mass, ammonia, and energy balances are entered on each component. Since there are loops in this cycle, the balances are coupled and the equations will be solved simultaneously. Starting at the pump.

$\dot{m}_1 = \dot{m}_2$

$\dot{m}_1 x_1 = \dot{m}_2 x_2$

$\dot{W}_{pump} = \dot{m}_2 h_2 - \dot{m}_1 h_1$

The pump power is the product of the volumetric flow rate and the pressure increase.

$$\dot{W}_{pump} = \frac{\dot{m}_1 v_1 (P_2 - P_1)}{\eta_{pump}}$$

Mass and ammonia balances on each of the two streams, an overall energy balance, and a heat transfer rate equation based on the known heat exchanger effectiveness are all required by the solutions heat exchanger (SHX).

$\dot{m}_2 = \dot{m}_3$

$\dot{m}_4 = \dot{m}_5$

$\dot{m}_2 x_2 = \dot{m}_3 x_3$

$\dot{m}_4 x_4 = \dot{m}_5 x_5$

$\dot{m}_2 h_2 - \dot{m}_4 h_4 = \dot{m}_3 h_3 - \dot{m}_5 h_5$

In order to calculate the heat transfer rate between the two streams, it is important to determine the minimum capacitance rate (the product of mass flow rate and specific heat) and apply the definition of heat transfer effectiveness.

$\dot{Q} = \varepsilon_{shx}\, \dot{C}_{min}\, (T_4 - T_2)$

where

$\dot{C}_{min} = \min(\dot{c}_{2\text{-}3}\, ,\, \dot{c}_{4\text{-}5})$

$C_{23} = \frac{(h_2 - h_3)}{(T_2 - T_3)}$, $C_{45} = \frac{(h_4 - h_5)}{(T_4 - T_5)}$, $\dot{C}_{2\text{-}3} = \dot{m}_2 c_{23}$, $\dot{C}_{4\text{-}5} = \dot{m}_4 c_{45}$

$\dot{Q}_{shx} = \dot{m}_2 (h_3 - h_2)$

$\dot{Q}_{shx} = \dot{m}_4 (h_4 - h_5)$

In order for these equations to be solved, a guess equation of $\dot{m}_4$ is used temporarily.

As the generator and rectifier are so closely coupled, it is best to enter and solve the equations for both components. Mass, ammonia, and energy balances on the generator result in;

$\dot{m}_3 + \dot{m}_8 = \dot{m}_7 + \dot{m}_4$

$\dot{m}_3 x_3 + \dot{m}_8 x_8 = \dot{m}_7 x_7 + \dot{m}_4 x_4$

$\dot{m}_3 h_3 + \dot{m}_8 h_8\, \dot{Q}_{gen} = \dot{m}_7 h_7 + \dot{m}_4 h_4$

For the rectifier,

$\dot{m}_7 = \dot{m}_9 + \dot{m}_8$

$\dot{m}_7 x_7 = \dot{m}_9 x_9 + \dot{m}_8 x_8$

$\dot{m}_7 x_7 = \dot{m}_9 h_9 + \dot{m}_8 h_8 + \dot{Q}_{rect}$

Reasonable results can be obtained with a simple approximation by making two assumptions: (1) assuming that the vapor leaving the generator (state 7) is in equilibrium with the liquid which is entering (state 3) and (2) that the liquid leaving the rectifier (state 8) is in equilibrium with the vapor which is entering (state 7). The first assumption represents the ideal counter-flow generator limiting case. The second assumption represents the reversible rectifier. When taken together, these conditions require

$T_8 = T_7$

$x_8 = x_3$

The specific enthalpy at state 8 is calculated from property relations while State 9 is assumed to be saturated vapor (quality = 1), and the pressure is known.

The guess equation of $\dot{m}_4$ is removed at this point. The mass and energy balances for the expansion valve between the solution heat exchanger and the absorber are written as

$\dot{m}_5 = \dot{m}_6$

$\dot{m}_5 x_5 = \dot{m}_6 x_6 \quad \rightarrow x_5 = x_6$

$\dot{m}_5 h_5 = \dot{m}_6 h_6 \quad \rightarrow h_5 = h_6$

The temperature and quality at state 6 are found using property relations. These equations are entered for the expansion valve and solved. The guess values are updated.

For the condenser, the balances are;

$\dot{m}_9 = \dot{m}_{10}$

$\dot{m}_9 x_9 = \dot{m}_{10} x_{10} \quad \rightarrow x_9 = x_{10}$

$\dot{Q}_{cond} = \dot{m}_9 h_9 - \dot{m}_{10} h_{10}$

At state 10 the condensate is assumed to be a saturated liquid, and the specific enthalpy is determined by property relations. To avoid an error in the software, the equation that was eneterd for x_{10} is removed.

Mass, ammonia, and energy balances for the refrigerant expansion valve between the condenser and the evaporator are as follows.

$\dot{m}_{10} = \dot{m}_{12}$

$\dot{m}_{10} x_{10} = \dot{m}_{12} x_{12} \quad \rightarrow x_{10} = x_{12}$

$\dot{m}_{10} h_{10} = \dot{m}_{12} h_{12} \quad \rightarrow h_{10=} = h_{12}$

The mass, ammonia, and energy balance for the evaporator are as follows. The temperature and quality at state 11 can be determined by property relations. The specific enthalpy at state 12 is also be determined by property relations.

$\dot{m}_{11} = \dot{m}_{12}$

$\dot{m}_{11} x_{11} = \dot{m}_{12} x_{12} \quad \rightarrow x_{11} = x_{12}$

$\dot{Q}_{evap} = \dot{m}_{12} h_{12} - \dot{m}_{11} h_{11}$

At this stage the temporary equation that was set for x_{11} is removed. The last component in the system is the absorber. The mass and ammonia balances for the absorber are redundant, since the mass flows are cyclic and mass and ammonia balances have been written for all other

components. It is recommended to introduce mass and ammonia error terms, as follows.

$\dot{m}_{12} + \dot{m}_6 = \dot{m}_1 + \Delta m$

$\dot{m}_{12}x_{12} + \dot{m}_6x_6 = \dot{m}_1x_1 + \Delta a$

Upon solving, the values of Δm and Δa should both be very close to zero. This confirms that the mass and ammonia balances on all components in the cycle are satisfied. The energy balance on the absorber determines the rate at which heat must be rejected from the absorber.

$\dot{m}_{12}x_{12} + \dot{m}_6x_6 = \dot{m}_1x_1 + \dot{Q}_{abs}$

The maximum geothermal fluid energy was then used as the input into both systems.

2.4 Compare the performance of the LiBr-water and NH3-water absorption systems for this application and choose the most suitable system.

The COPs of both systems were calculated and compared. Below is the equation that was used for calculating the COPs;

$$COP_{refrig} \approx \frac{Q_E}{Q_G + W_p}$$

2.5 Design an ARS suited for this application, providing optimized design features of the heat exchangers.

The LiBr-water ARS was found to be the more suited system for this application. Therefore, a LiBr-water ARS was designed. In the process of designing this system, A UA model was added to the internal model

2.5.1 UA model

The first stage in designing a UA model is updating the guess values in the internal model and then following the steps below for each component that involves the exchange of heat:

(1) Assuming a reasonable temperature difference in the outside water loop;

(2) Calculating the water mass flow rate that is consistent with that temperature difference and the known heat transfer rate;

(3) Calculating the UA value consistent with the temperatures and the heat transfer rates.

The results are given in a table once this is completed. However, the UA values and fluid loop mass flow rate values for each corner component given in this table are arbitrary values. The guess values to the current solution must be updated, once this is done the next step is to edit the input values to some more reasonable set. In going from the internal model to the UA model, the four internal cycle temperature inputs are replaced by four temperature inputs at the inlet to each of the four heat transfer fluid loops. Apart from the four temperature inputs, the fluid loops require specification of the mass flow rate of the fluid, the specific heat of the fluid, and the size of each heat exchanger (the UA value). The log mean temperature difference calculation performed in these models is implemented as a software (EES) function. This is convenient because the same calculation is repeated a number of times with different input values.

2.5.2 Simulations of the LiBr-Water absorption system.

In order to understand how a number of important parameters affects the absorption system and to optimize the system for it to perform the required function, a number of simulations for different parameters were done. Observations of the effects of each absorption parameter on system performance and other operational parameters were made for a specific amount of input heat into the generator (8.091kW) and cooling load (5.838kW). Some parameters that were varied in order to assess their effects on other absorption parameters Included; effects of Evaporator size (UA_e) on cooling capacity and COP, effect of external loop evaporator temperature on the absorption system, effect of generator external loop mass flowrate on the absorption system and effect of generator external loop inlet temperature on the absorption system.

2.5.3 LiBr-water absorption chiller complete designing

Having taken into consideration the results of the simulations and all other constraints. A LiBr-Water absorption system was designed for the storage of milk at a suitable storage temperature of 4ºC. The storage temperature is expected to fluctuate as various parameters of the system change. However, the system is designed to store milk between temperatures 3.60ºC and 4.4ºC. This design was built from the internal model solutions. Based on the values of heat absorbed or rejected by various components of the internal model and the desired inlet and outlet temperatures of all components. The external loop mass flowrate, Log mean temperature differences and UA values were calculated and used as inputs into the UA model. The UA model included the heat exchange of various components with external parameters such as external loop mass flowrates and external loop inlet and outlet temperatures.

3. RESULTS AND DISCUSSION

3.1 Thermodynamic analysis of each component of both absorption systems

The thermodynamic analysis of both absorption systems was done for each component; the generator, condenser, evaporator, absorber, solution pump and solution heat exchanger. Below are the results of the analysis based on the highest possible temperature input (80ºC) and the mass flow-rate (6kg). The state points of these results correspond to figures 2.1 and 2.2 respectively.

Table 3.1: LiBr-water system results

	h_i (J/kg)	m_i (kg/s)	Q_i	T_i (ºC)	x_i
1	75.3	4.950		30.00	0.5456
2	75.3	4.950		30.00	0.5456
3	129.9	4.950		56.60	0.5456
4	152.3	4.790		65.00	0.5637
5	95.9	4.790		37.00	0.5637
6	95.9	4.790		37.00	0.5637
7	2615.4	0.160		61.53	0
8	125.7	0.160		30.00	0
9	125.7	0.160	0.04701		0
10	2504.6	0.160		2.00	0

ε_{shx}=0.8 v_1=0.0006216 [m^3/kg]
P_H=4.247 [kPa] P_L=0.706 [kPa]

Description	symbol	value (kW)
Absorber heat rejected	$\dot{Q}_a$	486.5
Condenser heat rejected	$\dot{Q}_c$	397.5
Heat input to generator	$\dot{Q}_g$	504.2
Capacity	$\dot{Q}_e$	379.8
Solution heat exchange rate	$\dot{Q}_{shx}$	270.6
Pump work	$\dot{W}$	0.0108
Coefficient of performance	COP	0.7533

Table 3.2: NH_3-water system results

	h_i (J/kg)	m_i (kg/s)	Q_i	T_i (ºC)	x_i
1	-126.3	1.097	0	25.00	0.5341
2	-125.5	1.097		25.05	0.5341
3	-125.5	1.097		25.05	0.5341
4	67.09	0.9030	0	75.75	0.4341
5	104.1	0.9030		75.75	0.4341
6	104.1	0.9030	0.07921	48.96	0.4341
7	1388	0.1963	1	58.68	0.9941
8	27.17	0.00231	0	33.25	0.5341
9	1313	0.1940	1	33.25	0.9996
10	117.3	0.1940	0	25.00	0.9996
11	117.3	0.1940	0.1073	-4.376	0.9996
12	1232	0.1940	0.9750	-4.00	0.9996

ε_{shx}=0.8 η_{pump} = 1 v_1=0.001228 [m^3/kg]
P_H=1003 [kPa] P_L=363.4 [kPa]

Description	symbol	value (kW)
Absorber heat rejected	$\dot{Q}_a$	471.5
Condenser heat rejected	$\dot{Q}_c$	231.9
Heat input to generator	$\dot{Q}_g$	504.1
Capacity	$\dot{Q}_e$	216.2
rectifier exchange rate	$\dot{Q}_{rhx}$	17.79
Pump work	$\dot{W}$	0.8619
Coffiecient of performance	COP	0.4289

The results show that the highest possible value of input energy (504kW) is able to produce a cooling load of 379.8Kw For a LiBr-water ARS and 216.2kW for the NH_3-water ARS. The cooling load of the Ammonia system is lower compared to the LiBr-water absorption system. However, both systems produce a cooling load sufficient for cooling over 100 000L of milk from 35ºC to the suitable storage temperature of 4ºC daily. This far exceeds the daily collection of milk (1500L) which is done in the study area. The available mass flowrate and generator input temperature is more than sufficient for powering both absorption refrigeration systems to cool milk to an appropriate storage temperature.

3.2 Assessment of COPs for both absorption systems.

The table 3.3 shows the results of the system performance (COP) obtained from both ARSs based on identical cooling capacities. The models that were used for comparing the COPs of the two systems were downsized to lower cooling capacities

Table 3.3 COPs of both the LiBr-water and NH_3-water absorption systems different cooling capacities.

	NH_3-water system					LiBr-water system			
	Capacity	mass flowrate	generator heat input	COP		Capacity	mass flowrate	generator heat input	COP
1	40 kW	0.200kg/s	62.10kW	0.6439	1	40kW	0.5200kg/s	52.97kW	0.7533
2	80 kW	0.403kg/s	183.1kW	0.4373	2	80kW	1.043kg/s	102.2kW	0.7533
3	120kW	0.605kg/s	274.8kW	0.4373	3	120kW	1.560kg/s	158.9kW	0.7533
4	160kW	0.806kg/s	366.1kW	0.4373	4	160kW	2.090kg/s	212.9kW	0.7533

The results show that for the same cooling capacities the LiBr-water system always had a greater COP than the NH_3-water system. Other parameters which affect the operation of an absorption systems, such as the internal model mass flowrate and the heat input into the generator were also monitored along with the COPs. The results showed that;

(1) For the same cooling capacity, the LiBr-water system requires a greater mass flowrate at state 1 (Figure 2.1) than the NH_3-water system.

(2) For the same cooling capacity, the NH_3-water system required a greater heat input into the generator than the LiBr-water system.

Based on the results, it was clear that the LiBr-water absorption system was best suited for this application of cooling milk to its suitable storage temperature.

3.3 LiBr-water absorption system model.

The results which were initially obtained from the complete internal model are shown in table 3.4. The LiBr-water system in this part is modelled to have the capacity just enough to chill over 1500L of milk per day to a storage temperature of 3.60ºC. The LiBr-water system internal model calculations based on a generator inlet temperature of 80°C, mass flowrate of 0.1kg/s and a solution heat exchanger exit temperature of 57°C are shown in table 3.4.

Table 3.4: LiBr-water system internal model results features

	h_i (J/kg)	m_i (kg/s)	Q_i	T_i (°C)	x_i
1	75.3	0.100		30.00	0.5456
2	75.3	0.100		30.00	0.5456
3	129.9	0.100		56.60	0.5456
4	152.3	0.097		65.00	0.5637
5	95.9	0.097		37.00	0.5637
6	95.9	0.097		37.00	0.5637
7	2615.4	0.003		61.53	0
8	125.7	0.003		30.00	0
9	125.7	0.003	0.04701		0
10	2504.6	0.003		2.00	0

ε_{shx}=0.8 v_1=0.0006216 [m^3/kg]
P_H=4.247 [kPa] P_L=0.706 [kPa]

Description	symbol	value (kW)
Absorber heat rejected	$\dot{Q}_a$	9.829
Condenser heat rejected	$\dot{Q}_c$	8.031
Heat input to generator	$\dot{Q}_g$	10.19
Capacity	$\dot{Q}_e$	7.674
Solution heat exchange rate	$\dot{Q}_{shx}$	5.467
Pump work	$\dot{W}$	0.00022
Coefficient of performance	COP	0.7533

Table 3.5: LiBr-water system optimum design

	h_i (J/kg)	m_i (kg/s)	Q_i	T_i (°C)	x_i
1	62.800	0.100		27.58	0.5197
2	62.800	0.100		27.58	0.5197
3	126.10	0.100		57.38	0.5197
4	146.50	0.098		66.00	0.5311
5	81.800	0.098		35.26	0.5311
6	81.800	0.098		35.26	0.5311
7	2619.7	0.002		64.02	0.0000
8	151.80	0.002		36.24	0.0000
9	151.80	0.002	0.05486	3.590	0.0000
10	2507.5	0.002		3.590	0.0000
11		0.121		80.00	
12				65.55	
13		0.468		25.00	
14				28.61	
15		0.382		25.00	
16				28.30	
17		0.046		30.00	
18				3.600	

ε_{shx}=0.8 v_1=0.0006391 [m^3/kg]
P_H=6.028 [kPa] P_L=0.7905 [kPa]

Description	Symbol	Value (kW)
Absorber heat rejected	$\dot{Q}_a$	7.105
Condenser heat rejected	$\dot{Q}_c$	5.295
Heat input to generator	$\dot{Q}_g$	7.345
Capacity	$\dot{Q}_e$	5.054
Solution heat exchange rate	$\dot{Q}_{shx}$	6.336
Pump work	$\dot{W}$	0.003347
Coefficient of performance	COP	0.6881
Description	**parameter**	**value (kW/K)**
Absorber size	UA_A	1.654
Condenser size	UA_C	0.557
Generator size	UA_G	1.304
Evaporator size	UA_E	1.400
Solution heat exchanger size	UA_{SHX}	0.7781

5.3 Simulations of the LiBr-Water absorption system.

A series of calculations for different parameters were done in order to observe the effects of each absorption parameter on system performance for a given heat source and cooling load. The simulations were done from a LiBr-water absorption model whose generator external loop mass flowrate was 0.1kg/s, generator external loop inlet temperature 80°C and generator external loop outlet temperature 60°C. This choice was arrived at because these parameters gave the cooling capacity which was just greater than the amounts of milk collected in the study area. The results obtained from the simulations are shown below.

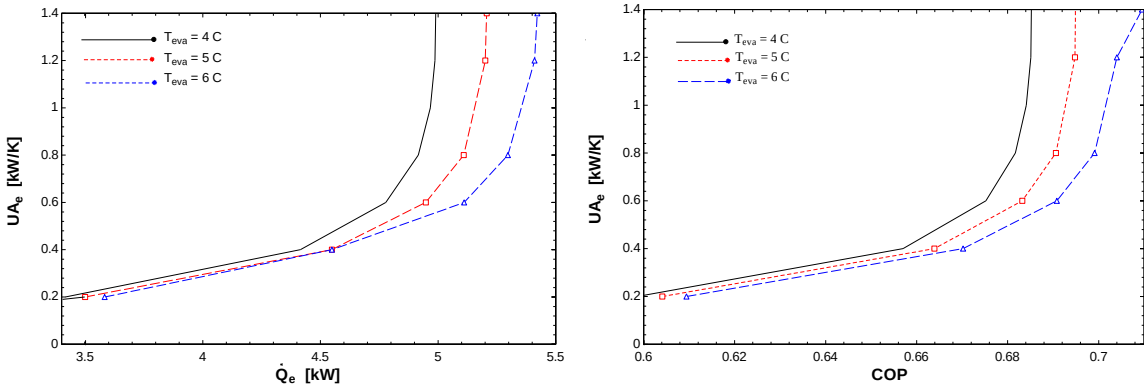

(a) effect of UA_e on system cooling capacity (b) effect of UA_e on system COP

Figure 3.1

The results show that as the UA values of the evaporator heat exchanger increased, the cooling capacity ($\dot{Q}_e$) and the COP both increased. Increasing the evaporator heat exchanger size also increases the capacity of the absorption system. The results also show that at higher evaporator temperatures, the capacity of the absorption system is higher for the same evaporator heat exchanger sizes. The effect of evaporator heat exchanger size on COP was similar, the COP of the

absorption system was observed to increase as the evaporator heat exchanger size is increased. The results also show that at higher evaporator temperatures, the COP of the system is higher for the same evaporator heat exchanger sizes.

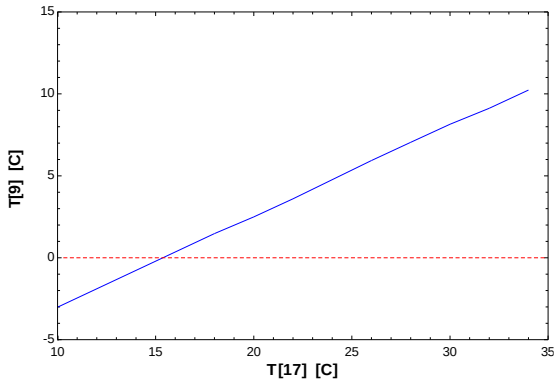

(a) Effect of external loop evaporator temperature on internal loop evaporator temperature.

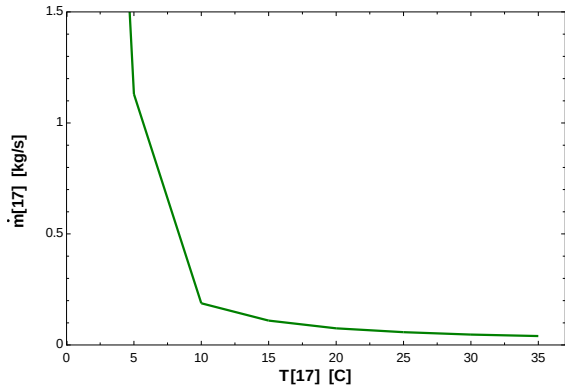

(b) Typical mass flowrates for specific values of external loop evaporator temperature.

Figure 3.2

It was observed that the internal loop evaporator temperature was directly proportional to the external loop evaporator temperature. As the external loop evaporator temperature decreased, the internal loop evaporator temperature also decreased. This created a problem in the absorption system. When the external loop evaporator temperature falls below 15^{o}C, the internal loop evaporator temperature falls to 0^{o}C (freezing point of water). The refrigerant temperature in this system must not be allowed to fall to 0^{o}C because the refrigerant (water) freezes at this temperature. When the refrigerant freezes, the absorption system is clogged and the system stops functioning. More simulations were run in order to find solutions and to prevent the internal evaporator temperature from falling to the freezing point of the refrigerant (water). The results of the simulations show that when the external loop evaporator mass flowrate is increased as the external loop evaporator temperature is reducing. The internal loop evaporator temperature can be controlled to stay within acceptable values above 0^{o}C. After running these simulations the external loop evaporator mass flowrates corresponding to specific external loop evaporator temperatures, able to keep the internal loop evaporator temperature at 3.87^{o}C throughout the cooling process were found. The results are shown in figure 3.2(b).

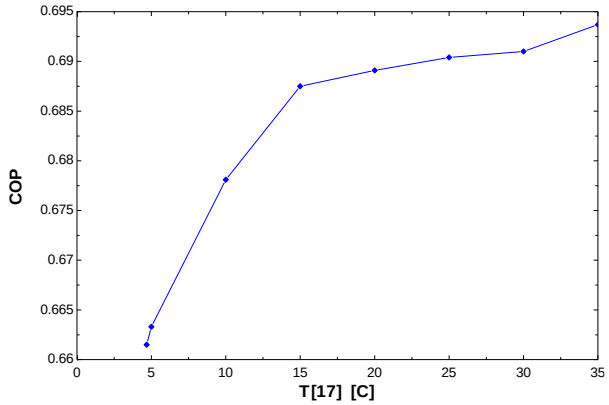

(a) effect of external loop evaporator temperature on COP

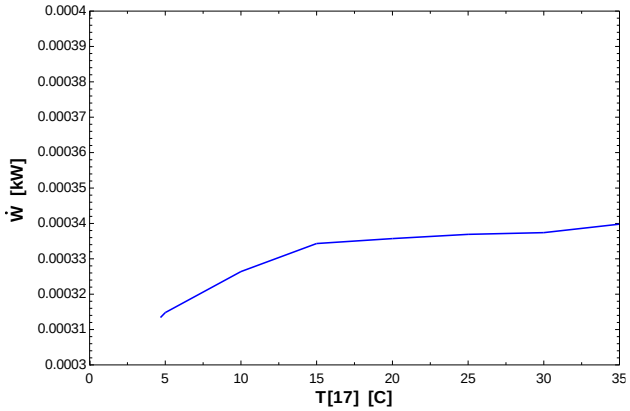

(b) effect of external loop temperature on pump work

Figure 5.3

The results of this simulation shows that the COP increases as the external loop evaporator temperature increases. The pump work was also slightly affected by the external loop evaporator temperature, it increased slightly as the external loop evaporator temperature is increasing.

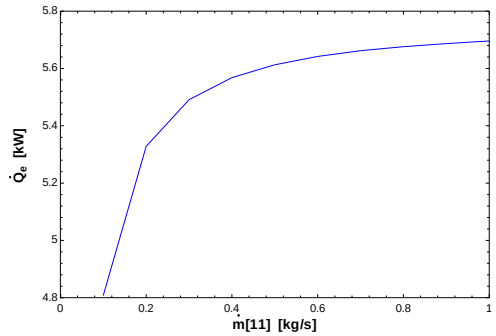

(a) Typical effect of generator external loop mass flowrate on cooling capacity.

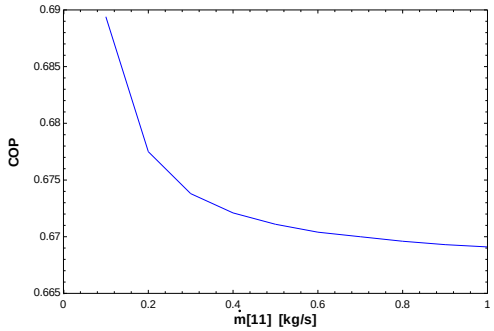

(b) Typical effect of generator external loop mass flowrate on the coefficient of performance.

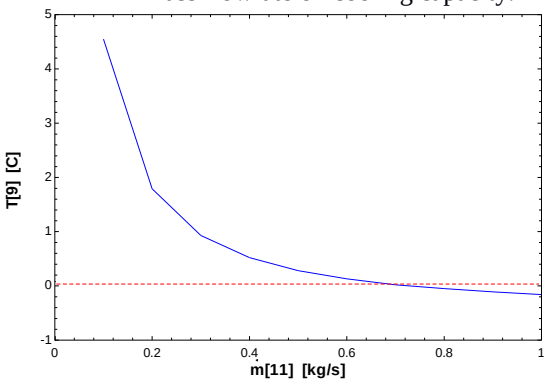

(c) Typical effect of generator external loop mass flowrate on the evaporator temperature.

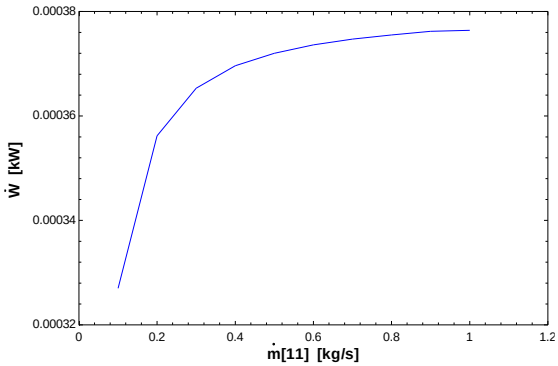

(d) Typical effect of generator external loop mass flowrate on the pump work

Figure 3.4

The simulations here were run to determine the effect of generator external loop mass flowrate on various absorption parameters. The results show that increasing the generator external mass flowrate affects various absorption parameters differently.

(1) The cooling capacity of the absorption system increases when the generator external loop mass flowrate is increased, figure 3.4 (a).

(2) The COP of the absorption system decreases when the generator external loop mass flowrate is increased, figure 3.4 (b).

(3) The internal loop evaporator temperature also decreases as the generator external loop mass flowrate is increased, figure 3.4 (c). Further, when the generator mass flowrate goes beyond 0.70kg/s, the evaporator temperature falls to 0^{o}C (the refrigerant freezing point). This cannot be allowed to happen as it would freeze the refrigerant and clog the system. Therefore, for the capacity of the LiBr-water absorption designed in this study, the generator external loop mass flowrate should be prevented from going beyond 0.7kg/s while the other features remain the same.

(4) The internal loop pump work slightly increases as the generator external loop mass flowrate is increased. To avoid these changes in pump work, the generator external loop mass flowrate must be kept constant.

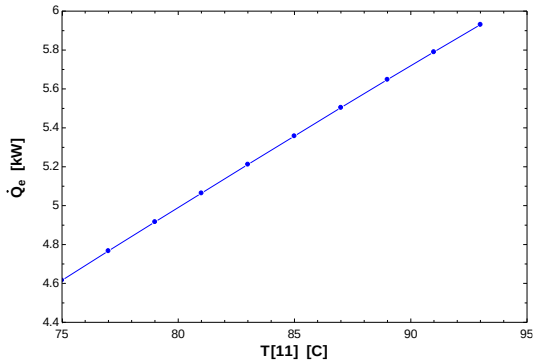

(a) Typical effect of generator external loop temperature on cooling capacity.

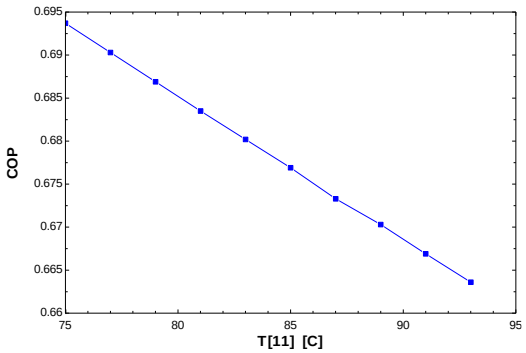

(b) Typical effect of generator external loop temperature on COP.

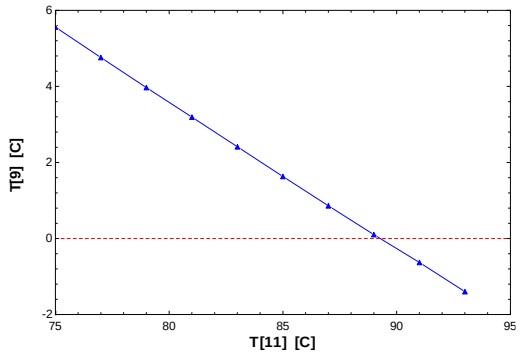

(c) Typical effect of generator external loop temperature on evaporator temperature.

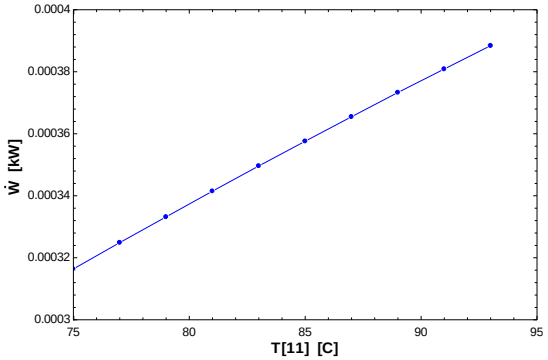

(d) Typical effect of generator external loop temperature on pump work.

Figure 3.5.

The results these simulations show that increasing the generator external temperature affects various absorption parameters differently.

(1) The cooling capacity of the absorption system varies directly as the generator external loop temperature, figure 3.5 (a).

(2) The COP of the absorption system varies inversely as the generator external loop temperature, figure 3.5 (b).

(3) The evaporator temperature also varies inversely as the generator external loop temperature, figure 3.5 (c). It must be noted that when the generator external loop temperature exceeds 89^{o}C, the evaporator temperature falls to 0^{o}C (the refrigerant freezing point). This cannot be allowed to happen as it would freeze the refrigerant and clog the system. The results show that the generator external loop temperature must be kept between 77^{o}C and 83^{o}C in order to keep the milk at suitable storage temperatures while also maintaining the proper operation of the absorption system.

(4) The pump work varies directly as the generator external loop temperature but only slightly, the pump work did not increase or reduce by much as the generator external loop temperature was increased.

5.4 LiBr-water absorption chiller design specifications.

Based on the values of heat absorbed or rejected by various components of the internal model and the desired inlet and outlet temperatures of all components. The external loop mass flowrate, Log mean temperature differences and UA values were calculated and used as inputs into the UA model. The UA model included the heat exchange of various components with external parameters such as external loop mass flowrates and external loop inlet and outlet temperatures. The design features obtained produced a cooling effect but not enough to cool the milk to the storage temperature of 4^{o}C. The system was then optimized so that it is able to cool milk to the suitable storage temperature. This was done by taking into consideration the results from the simulations. A number of parameters were changed until the absorption system produced the desired results, the optimized design features are shown in table 3.5.

4. CONCLUSIONS

The conclusions arising from this investigation are outlined below:

1. The exhaust geothermal fluid from the ORC machine at the Bwanda and Gwisho hotsprings geothermal site contains enough energy (504kW) to power both types of absorption systems for storing the amounts of milk collected per day (1500L) in the study area to a suitable storage temperature of 4^{o}C. Further, the results show that the LiBr-water system gives a larger cooling capacity (379.8 kW) than the NH_3-water system (216.2kW) at the same generator input energy (504kW). This means that the LiBr-water system can be used to store much larger volumes of milk compared to the NH_3-water system for the same input energy into the generator.
2. For the same cooling capacities (40kW, 80kW, 120kW, 160kW), the COP of the LiBr-water absorption system is always higher (0.7533) compared to that of the NH_3-water system (0.4373 – 0.64390). The COP of the NH_3-water system increases slightly for low cooling capacities.
3. The LiBr-water absorption refrigeration system is the most suited system for the application in this study because of the first two conclusions. It was noted during the design and simulation process that the absorption refrigeration system should be designed properly in order to achieve its peak performance since different amounts of heat input and cooling load affects absorption parameters. Fine tuning the external loop evaporator mass flowrate and evaporator heat exchanger size ensures that the internal loop evaporator does not fall to the refrigerant freezing point during cooling.

The results also showed that the NH_3-water system requires much more input energy (62.10 kW - 366.1kW) into the generator than the LiBr-water system (52.97 kW - 212.9kW) for the same cooling capacities (40kW – 160kW), and the

pump work of the NH_3-water system is always higher than that of the LiBr-water system. This implies that the NH_3-water system will require a larger amount of electrical energy to operate for the same cooling capacity compared to the LiBr-water system. The advantage of a NH_3-water absorption system is that it can operate far below 0°C, LiBr-water system cannot operate under 0^oC because the freezing point of its refrigerant (water) is 0^oC. For applications that require suitable storage temperatures which fall below 0^oC, the NH_3-water absorption system is the most suited absorption system.

REFERENCES

1. Ministry of Energy (MoE), Renewable energy strategy and action plan, Lusaka, Zambia. 2022.
2. Kalahari geoenergy, Energy beyond power, 2022.
3. A. O'Connell, P.L. Ruegg, K. Jordan, B. O'Brien and D. Gleeson, 2016. The effect of storage temperature and duration on the microbial quality of bulk tank milk. Journal of Diary Science, Volume 99 (Issue 5), pp. 3367-3374.
4. R. Kumar, Research methodology - a step by step guide. third edition. New Dhelhi: Sage publications, 2011.
5. K. E. Herold, R. Radermacher, S. A. Klein, absorption chillers and heat pumps, second edition, CRC press: New York, 2016.
6. Tesha, Absorption refrigeration system as an integrated condenser cooling unit in a geothermal power plant, 2009.
7. US Department of Energy, Energy Efficiency and Renewable Energy, Combined Heat and Power Technology Fact Sheet Series, May 2017.
8. M. A. Nazari, A. Mukhtar, A. Shah, H. Yasir, M. H. Ahmadi, R. Kumar and T. Luong, 2024. Applications of geothermal sources for absorption chillers as efficient and clean cooling technologies for buildings: A comprehensive review. Journal of building engineering, 82(108340).
9. M. El Haj Assad, M. Albawab, M. Tawalbeh, A. Khosravi, Z. Said, Thermodynamic analysis of geothermal series flow double-efffect water/LiBr absorption chiller, 2019.
10. Ministry of energy (MoE), Zambia energy efficiency strategy and action plan, 2022.